Signatures of HyperCharge Axions in Colliders

Ram Brustein, David H. Oaknin

Department of Physics, Ben-Gurion University, Beer-Sheva 84105, Israel

email: ramyb, doaknin @bgumail.bgu.ac.il

Abstract

If in addition to the standard model fields, a new pseudoscalar field that couples to hypercharge topological number density, the hypercharge axion, exists, it can be produced in colliders in association with photons or Z bosons, and detected by looking for its decay into photons or Z's. For a range of masses below a TeV and coupling above a fraction of 1/TeV, existing data from LEP II and the Tevatron can already put interesting constraints, and in future colliders accessible detection range is increased significantly. The hypercharge axion can help in explaining the matter-antimatter asymmetry in the universe.

If in addition to the standard model fields, a new pseudoscalar field that couples to hypercharge topological number density, the hypercharge axion (HCA), exists, it can be produced in colliders in association with photons or Z bosons. Since the hypercharge photon is a linear combination of the ordinary photon and the Z, HCA couples to photons and Z's and therefore it can be produced in interactions involving photons or Z's, and it can be detected by looking for its decay into photons or Z's. We show that HCA can be produced in colliders in sufficient numbers to be detected if its mass is below a few TeV and its coupling above a fraction of TeV^{-1}. In cosmology, HCA can exponentially amplify hypercharge fields in the symmetric phase of the electroweak plasma, while coherently rolling or oscillating [1,2], leading to the formation of a time-dependent condensate of topological number density. This condensate can be converted at the electroweak phase transition [3], under certain conditions, into baryons in sufficient quantity to explain the observed baryon asymmetry in the universe [1].

Pseudoscalar fields with the proposed axion-like coupling appear in several possible extensions of the Standard Model (SM) [4]. They typically have only perturbative derivative interactions and therefore vanishing potential, and acquire a mass m, which could be as low as a fraction of an eV, or as high as 10^{12} GeV, through non-perturbative interactions. The scale of mass generation F, could be as high as the Planck scale but could also be much lower, even down to the TeV range, however, typically $m \ll F$. A particularly interesting mass range is the TeV range, expected to appear if mass generation is associated with supersymmetry breaking, and if HCA plays a role in baryogenesis [1]. We focus on a singlet elementary HCA whose only coupling to SM fields is to hypercharge fields, but composite or non-singlet fields may also appear in some models [4].

The singlet HCA field X has mass m_X, and the following dimension 5 interaction Lagrangian density,

$$\mathcal{L}_{XYY} = \frac{1}{8M}\, X \epsilon^{\mu\nu\rho\sigma} Y_{\mu\nu} Y_{\rho\sigma}\,, \tag{1}$$

where $Y_{\mu\nu}$ is the $U(1)_Y$ hypercharge field strength, and the coupling $\frac{1}{M}$ has units of mass^{-1}.

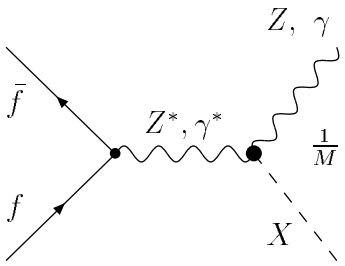

FIG. 1. Associated production of HCA in colliders. The fermions f can be either charged leptons or quarks.

For QCD axions, $M \sim F$, F being the "Peccei-Quinn" mass generation scale. But in general, it is not always the case, and we will therefore take M to be a free parameter, and in particular allow $M < F$, keeping the characteristic property $m_X \ll M$. We will be interested in a range $M < 100$ TeV, and $m_X < 10$ TeV. Our model is therefore a two parameter model, and the goal of our subsequent analysis is to determine for which domain in (m_X, M) space, HCA can be produced and detected in colliders.

The interaction (1) is not renormalizable, and therefore our model should be considered as an effective field theory, with a cutoff. We may estimate the magnitude of radiative corrections to SM quantities, such as the ρ parameter, to check that our model is consistent with existing electroweak measurements, which require additional corrections to be smaller than a fraction of a percent. The relative magnitude of a loop with external gauge bosons and an internal X particle, compared to the same process at tree level is approximately of order $\frac{1}{16\pi^2}\frac{m_X^2}{M^2}$, assuming that X is the heaviest particle running in the loop [5]. However, according to our assumptions $m_X \ll M$, and therefore expected radiative corrections are small. We will not attempt here a more detailed treatment of radiative corrections.

HCA can be produced in colliders, if the energy is high enough, in association with a photon or a Z. Recall that the hypercharge photon Y_μ is a linear combination of the ordinary photon A_μ and the Z boson Z_μ, $Y_\mu = \cos\theta_W A_\mu - \sin\theta_W Z_\mu$, where θ_W is the Weinberg angle. The total unpolarized cross sections for the two processes $f\overline{f} \to Z^*, \gamma^* \to ZX$ and

	e	Up type quarks	Down type quarks
c_v	$-\frac{1}{2}+2\sin^2\theta_W$ $\simeq -0.03$	$\frac{1}{2}-\frac{4}{3}\sin^2\theta_W$ $\simeq 0.19$	$-\frac{1}{2}+\frac{2}{3}\sin^2\theta_W$ $\simeq -0.34$
c_a	$-\frac{1}{2}$	$\frac{1}{2}$	$-\frac{1}{2}$
N_c	1	3	3

TABLE I. Parameter values for different fermions.

$f\overline{f} \to Z^*, \gamma^* \to \gamma X$, (here Z^* and γ^* denote a virtual Z and a virtual photon, and f is a charged fermion) can be computed from the diagrams in Fig. 1,

$$\sigma(f\overline{f} \to ZX) = \frac{1}{N_c}\frac{\alpha}{48}\frac{1}{M^2}\frac{k^{3/2}}{s}\frac{\sin^2\theta_W}{\cos^2\theta_W} \times \left(\left[\frac{\frac{1}{2}(c_v-c_a)}{s-M_z^2}+\frac{\cos^2\theta_W}{s}\right]^2+\left[\frac{\frac{1}{2}(c_v+c_a)}{s-M_z^2}+\frac{\cos^2\theta_W}{s}\right]^2\right), \tag{2}$$

$$\sigma(f\overline{f} \to \gamma X) = \frac{1}{N_c}\frac{\alpha}{48}\frac{1}{M^2}\frac{q^{3/2}}{s} \times \left(\left[\frac{\frac{1}{2}(c_v-c_a)}{s-M_z^2}+\frac{\cos^2\theta_W}{s}\right]^2+\left[\frac{\frac{1}{2}(c_v+c_a)}{s-M_z^2}+\frac{\cos^2\theta_W}{s}\right]^2\right), \tag{3}$$

where $k=(s-m_X^2-m_Z^2)^2-4m_X^2m_Z^2$, $q=(s-m_X^2)^2$ and $\sqrt{s}$ is center of mass (CM) energy of the collision. In deriving eqs.(2,3) we have assumed that the fermions are effectively massless, $m_f/\sqrt{s} \ll 1$. The parameters appearing in eqs.(2,3) are given in Table I: c_v and c_a are the vector and axial coupling of the fermion to the Z, N_c is the number of colors of the fermion, and takes into account averaging over initial colors. Notice that for small s there are kinematical thresholds for both processes, $s > m_X^2$, $s > (m_X+m_Z)^2$ to allow associated production with a photon, and with a Z, respectively.

In Fig. 2 we plot the total cross section for associated production of HCA in e^+e^- colliders as a function of CM energy $\sqrt{s}$, for $m_X = 150$ GeV, and $M = 1$ TeV. The cross section scales as M^{-2}, and therefore its magnitude for different values of M can be read

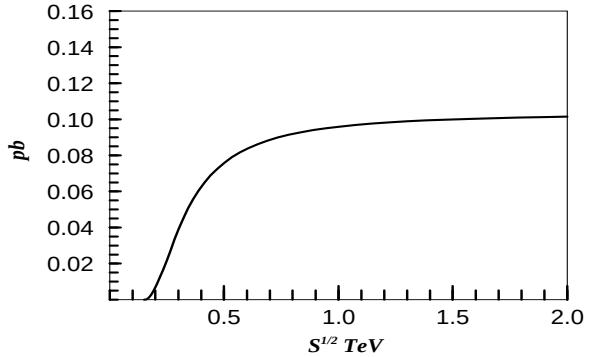

FIG. 2. Total HCA associated production cross section in e^+e^- colliders, for $m_X = 150$ GeV, $M = 1$ TeV.

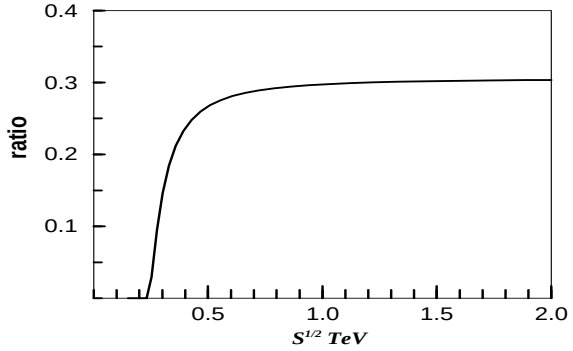

FIG. 3. Ratio of cross section for associated production of HCA with a Z boson, to cross section for associated production of HCA with a photon in e^+e^- colliders, for $m_X = 150$ GeV.

off Fig. 2. Since $q^{3/2}, k^{3/2} \sim s^3$ for large s, both cross sections approach asymptotically a constant independent of the mass m_X [6], $\sigma(f\overline{f} \to ZX) \to \frac{1}{N_c}\frac{\alpha}{48}\frac{1}{M^2}\tan^2\theta_W S_f$ and $\sigma(f\overline{f} \to \gamma X) \to \frac{1}{N_c}\frac{\alpha}{48}\frac{1}{M^2}S_f$, where S_f is a numerical factor of order unity depending on the type of fermion. The rise towards the asymptotic value is governed by the ratios m_X^2/s, and m_Z^2/s. Asymptotically, for large s, $\frac{\sigma(f\overline{f}\to ZX)}{\sigma(f\overline{f}\to\gamma X)} \simeq \tan^2\theta_W \simeq 0.3$. The ratio of associated production cross section with a Z to associated production cross section with a photon in e^+e^- colliders is shown in Fig. 3 for $m_X = 150$ GeV. The ratio is, of course, independent of M.

To evaluate the cross section in hadron colliders such as the Tevatron and LHC we follow the standard procedure of calculating hadronic cross section $\sigma_{hadrons}$, for hadron collisions at CM energy $\sqrt{s}$, from partonic ones $\hat{\sigma}_{ij}$ [7,8], $\sigma_{hadrons} = \int \sum_{ij} f_i^{(a)}(x_1, Q^2) f_j^{(b)}(x_2, Q^2)\hat{\sigma}_{ij}(\sqrt{Q^2})dx_1 dx_2$, where $f_i^{(a)}$ and $f_j^{(b)}$ are the partonic structure functions of type-i and type-j quarks in type-(a) and type-(b) hadrons, respectively, x_1, x_2

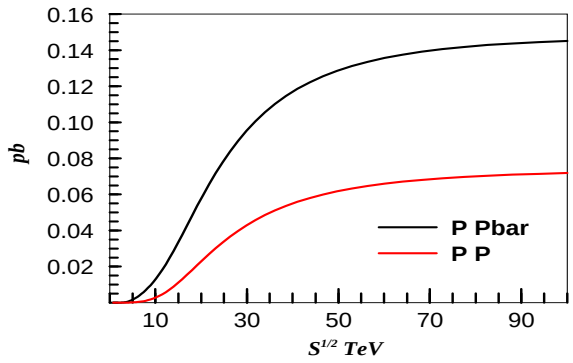

FIG. 4. Total HCA associated production cross section in hadronic colliders, for $m_X = 800$ GeV, $M = 1$ TeV.

are momentum fractions carried by partons 1 and 2, and $Q^2 = x_1 x_2 s$ is a typical momentum transfer in a partonic collision. For our process the only possible contributions are from the 6 same-flavour quark-antiquark partonic collisions, whose cross section is given in eqs.(2,3). Typically, the hadronic cross section for a $P\bar{P}$ or a PP machine is similar to an e^+e^- machine at about 0.1 CM energy. The hadronic cross section of a PP machine is suppressed with respect to the cross section in a $P\bar{P}$ machine by an additional factor associated with light antiquarks density within the proton. In Fig. 4 we show the results of numerically evaluating total hadronic cross section for associated production of HCA of mass $m_X = 800$ GeV, for $M = 1$ TeV. The ratio of associated production cross section with a Z to associated production cross section with a photon in $P\bar{P}$ and PP collisions, for the same parameters is shown in Fig. 5. As previously noted, the rise towards the asymptotic value is governed by the ratios $m_X^2/\tilde{s}$, and $m_Z^2/\tilde{s}$, where $\sqrt{\tilde{s}} \sim 0.1\sqrt{s}$ is the typical invariant mass of the partonic collisions. For small $\tilde{s}$ there are kinematical thresholds for both processes, $\tilde{s} > m_X^2$, $\tilde{s} > (m_X + m_Z)^2$, to allow associated production with a photon, and with a Z, respectively. The cross section scales as M^{-2}, and therefore its magnitude for different values of M can be read off Fig. 4.

Finally, we present the estimated number of produced HCA's in colliders. The total number of HCA produced N_{HCA}, is given by $N_{HCA} = \mathcal{L} \cdot \left(\frac{TeV}{M}\right)^2 \cdot \sigma\left(M = 1\ TeV; s; m_X\right)$, where $\mathcal{L}$ is the total integrated luminosity available. If we fix a number of events as the minimal number N^{min} required for detection of HCA, we obtain a region in (m_X, M) space, limited by the curve

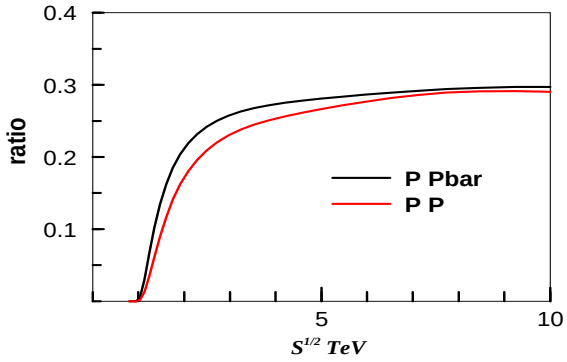

FIG. 5. Ratio of cross section for associated production of HCA with a Z boson, to cross section for associated production of HCA with a photon in hadronic colliders, for $m_X = 800$ GeV.

$$\frac{M}{TeV} = \sqrt{\frac{\mathcal{L}}{N^{min}}}\sqrt{\sigma\left(M = 1\ TeV; s; m_X\right)}, \tag{4}$$

shown in Fig. 6 for $N^{min} = 10$ events for LEP II and for Run I of the Tevatron collider. Existing experimental searches [9], have set upper bounds only on the cross section $\sigma(e^+e^- \to XZ)$, of the order of $0.1pb$, for $m_X < 90$ GeV, assuming that $X \to \gamma\gamma$ (see later). In Fig. 6, we have shown the excluded region in (m_X, M) space, assuming a uniform upper bound of $0.1pb$, for $10GeV < m_X < 90GeV$. We expect a better reach by a specialized analysis adapted to our model. At the Tevatron some analysis was performed [10] but the results are presented in a way that is not directly useful. The reach of future colliders is shown in Fig. 7, where we have fixed $N^{min} = 10$ events. For the graphs in Figs. 6, 7, we have chosen some generic parameters characterizing the various machines, summarized in Table II, but since graphs scale with parameters as in eq.(4), it is easy to adapt them to different parameters. In the region below the curve more than 10 events are expected with luminosities given in Table II, while in the region above the curve less than 10 events are expected. The vertical position of the curve scales as the square root of the integrated luminosity. Our choice of $N^{min} = 10$ events is motivated by our assumption that the SM background for our process is small (see below). Since curves in Figs. 6, 7, scale as $1/\sqrt{N^{min}}$, it is easy to determine the reach for different values of N^{min}.

collider	type	integrated luminosity	$\sqrt{s}$
LEP II	e^+e^-	$200pb^{-1}$	200 GeV
NLC	e^+e^-	$20fb^{-1}$	1 TeV
Tevatron	$P\bar{P}$	Run I: $100pb^{-1}$	1.8 TeV
		Run II: $2fb^{-1}$	2 TeV
		Run III: $30fb^{-1}$	2 TeV
LHC	PP	$20fb^{-1}$	14 TeV

TABLE II. Parameter values for different colliders.

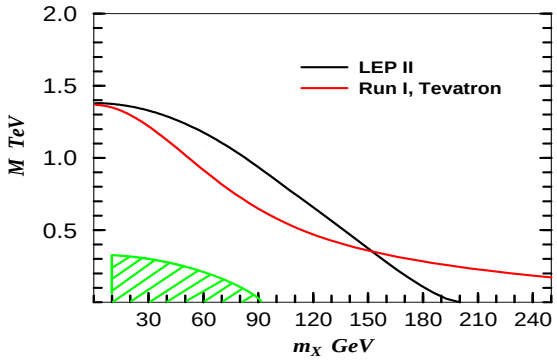

FIG. 6. Expected number of HCA's in LEP II, and Run I of the Tevatron. The curves correspond to 10 expected events, below (above) the curve more (less) than 10 events are expected. The shaded region is experimentally excluded.

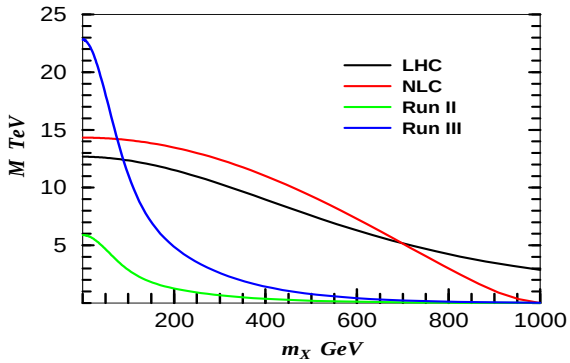

FIG. 7. Expected number of HCA's in future colliders. The curves correspond to 10 expected events, below (above) the curve more (less) than 10 events are expected.

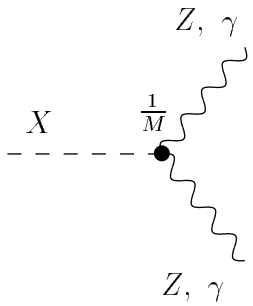

FIG. 8. Decay of HCA.

The produced HCA's decay into photons or Z's in rates that can be evaluated from the diagrams in Fig. 8. If $m_X < m_Z$, HCA can only decay into two photons, with a rate Γ given by $\Gamma(X \to 2\gamma) = \frac{1}{32\pi}\cos^4\theta_W \frac{m_X^3}{M^2}$. If $m_Z < m_X$, HCA has an additional decay channel, $\Gamma(X \to Z\gamma) = \frac{1}{32\pi}\cos^2\theta_W \sin^2\theta_W \left(\frac{(m_X^2-m_Z^2)^3}{m_X^3}\frac{1}{M^2}\right)$. Finally, if $m_X > 2m_Z$, HCA can also decay into two Z's, $\Gamma(X \to 2Z) = \frac{1}{32\pi}\sin^4\theta_W \frac{1}{M^2}(m_X^2 - 4m_Z^2)^{3/2}$. The total decay rate is the sum of rates for all the possible decay channels. The signature of a decay of HCA is therefore, depending on the mass m_X, a diphoton, photon Z or a ZZ systems in definite ratios.

The actual reach of colliders will be determined by the background to our process. In the SM there are no tree level processes leading to a final state with three neutral gauge bosons, which is the signature of our process. But there are one loop processes, which do lead to a final state with three neutral gauge bosons [11]. However, they do not seem to provide substantial background for values of M below 50 TeV. We will not attempt here a more detailed treatment of backgrounds.

If NLC can be operated as a photon collider, and its CM energy can be tuned, then HCA can be produced directly, through the reverse process of the one shown in the diagram in Fig. 8. The cross section for resonant production of X in photon colliders $\sigma = \frac{\pi}{4}\cos^4\theta_W \frac{1}{M^2} \sim 150\left(\frac{TeV}{M}\right)^2 pb$, is substantially larger than associated production cross section in e^+e^- colliders, and we believe that this option should be investigated further.

Our conclusions are that existing data from LEP II and Run I of the Tevatron can be used to rule out a region in (m_X, M) parameter space, as shown in Fig. 6, however a specific analysis, similar to the analysis performed in [9], but with the particular details of our model, has to be carried out to determine the exact region. In future colliders HCA can be detected provided that its mass is not too high, and its coupling is not too weak as shown in Fig. 7. The signature of HCA are events with 3 neutral gauge bosons (γ or Z), such as diphoton dijet events. Production of Z's requires higher energy, but once enough energy is available (see Figs. 2,4), and if the mass m_X is high enough, all possibilities will show up, with definite calculable reduction factors of 0.3 or smaller for each additional Z. The measured ratios can serve as a powerful check for verifying discovery. Higher effective luminosity increases the reach in coupling M, while higher energy increases the reach in mass m_X. In particular, for luminosities and energies given at Table II, LHC and NLC have a similar reach. In comparison, Run III of the Tevatron has a better reach in M for smaller m_X, and worse reach in m_X for smaller M.

HCA can play a role in baryogenesis only for a certain range of parameters, in particular, being conservative $m_X < 10$ TeV, while M appears only in combination with the initial coherent HCA amplitude, and is therefore not constrained directly. Detection of HCA in colliders with a mass below 10 TeV will support the hypothesis that HCA can help in explaining the observed matter - antimatter asymmetry in the universe.

ACKNOWLEDGMENTS

We gratefully acknowledge stimulating and useful discussions with G. Kane, and we thank G. Eilam for discussions about radiative corrections and photon colliders and M. Oreglia for comments about [9]. Work supported by the Israeli science Foundation. D.O. is supported by the Ministry of Education and Science of Spain.

REFERENCES

[1] R. Brustein and D.H. Oaknin, Phys. Rev. Lett. **82** (1999) 2628; hep-ph/9901242.

[2] E.I. Guendelman and D.A. Owen, Phys. Lett. **B276** (1992) 108.

[3] M. Giovannini and M.E. Shaposhnikov, Phys. Rev. Lett. **80** (1998) 22; C. Thompson, Phys. Lett. **B422** (1998) 61.

[4] M. Dine, P. Huet, R.J. Singleton and L. Susskind, Phys. Lett. **B257** (1991) 351.

[5] See, for example, A. Pich, hep-ph/9806303.

[6] Apart from a logarithmic dependence of $\alpha(\sqrt{s})$.

[7] E. Eichten, I. Hinchliffe, K. Lane and C. Quigg, Rev. Mod. Phys. **56** (1984) 579.

[8] C. Caso *et al.*, Eur. Phys. J. **C3** (1998) 1.

[9] K. Ackerstaff *et al.* [OPAL Collaboration], Phys. Lett. **B437**, 218 (1998).

[10] F. Abe *et al.* [CDF Collaboration], Phys. Rev. Lett. **81**, 1791 (1998); B. Abbott *et al.* [D0 Collaboration], Phys. Rev. Lett. **82** (1999) 2244; P.J. Wilson [CDF Collaboration], preprint Fermilab-Conf-98/213-E.

[11] G. Jikia, Nucl. Phys. **B405**, 24 (1993); G. Jikia and A. Tkabladze, Phys. Lett. **B323**, 453 (1994); Phys. Lett. **B332**, 441 (1994).